XI International Conference on Computational Methods in Marine Engineering

Drag Loads to Aquaculture Nets and the Corresponding Flow Velocity Reduction Behind

Are Johan Berstad

Aquastructures, Kjøpmannsgata 21 7013 Trondheim Norway. www.aquastructures.no.

Corresponding author are@aquastructures.no

ABSTRACT

Aquaculture nets, critical for fish containment, experience significant drag loads influenced by net solidity. Standardized photographic methods, per NS 9415 (2021), have improved solidity measurements, while increased empirical data have enabled refined drag models. This paper presents how drag not nets analysis models in AquaSim have been modified. By integrating 1D momentum theory from wind turbine blade element momentum (BEM) methods with the drag model of Berstad et al. (2012), we derive an updated expression for net drag and a new formula for flow reduction behind nets. Comparisons with empirical data from Moe Fore et al. (2022) and Marchand et al. (2024) show that the AquaSim 2025 model closely matches observed drag coefficients across a range of solidities, outperforming the 2012 formulation. Being less conservative, the model requires accurate input solidity for reliable results, improving the accuracy of computational simulations for safer and more efficient aquaculture structures. The momentum theory also leads to an expression for flow reduction behind nets which is an update of the current calculation of flow reduction based on Løland (1991). The method, 'the energy method' replaces the earlier model.

Figure 1 Typical fish farm.

Keywords: Aquaculture, Net, Drag, Flow Reduction, Computational Methods, Solidity

1 INTRODUCTION

Aquaculture, a key contributor to global seafood production, is mostly produced in nets within moored circular collars to contain fish as shown in Figure 1. These nets face significant hydrodynamic challenges, including drag loads, which affect structural integrity and operational safety. Regulations and standards like NYTEK and NS 9415 (2021) mandate robust net designs, with NS 9415 standardizing solidity measurements and setting criteria for structural and environmental safety to prevent fish escapes.

Accurate modeling of drag loads, driven by net solidity, is critical for aquaculture infrastructure. U Until 2025, AquaSim, the leading numerical tool, simulates these loads using formulations from Berstad et al. (2012) for drag load to a net and Løland (1991) for flow reduction behind nets. This paper advances AquaSim by adapting one-dimensional momentum theory (Rankine 1865), to improve drag and flow reduction models for nets. This novel approach, validated against empirical data, enhances the precision of computational simulations, supporting safer and more efficient aquaculture designs in alignment with marine engineering advancements.

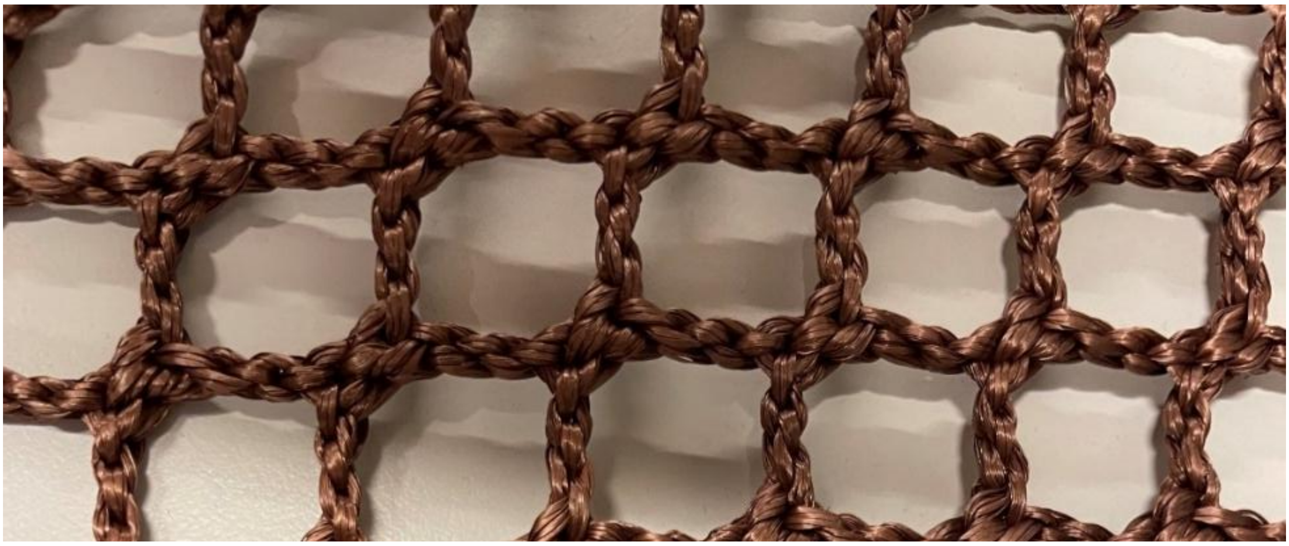

Figure 2 Netting example.

2 SYMBOLS

Symbol	Description	Units
A	Area	m²
A_tot	Total area of a net panel	m²
A_e	Projected area of net twines	m²
F	Force (e.g., drag force F_drag, equivalent to thrust T)	N
L	Length (e.g., mesh side length)	m
Sn	Solidity, ratio of projected twine area to total net panel area, equivalent to σ in Hansen (2008)	Dimensionless
a	Induction factor, relates flow velocity at net (u) to undisturbed velocity v: $u = v(1-a)$	Dimensionless
d	Diameter of net twine	m
k	Factor accounting for knot effects in net solidity, typically 1 or 2	Dimensionless
r	Reduction factor, ratio of velocity behind net (v_{red}) to undisturbed velocity (v)	Dimensionless

u	Flow velocity at net	m/s
u^*	Velocity at panel relative to undisturbed velocity, used in Steiros et al. (2018)	Dimensionless
v	Undisturbed free-stream velocity upstream of net	m/s
v_{red}	Reduced flow velocity behind net	m/s
φ	Inflow angle, where 90° is perpendicular to net panel	Degrees
ρ	Fluid density	kg/m³
Cd	Drag coefficient. Variants include: Cd_{cyl} (single cylindrical twine), Cd_{mem} (net relative to projected twine area), Cd_{2012} (AquaSim 2012), *Cd_E1*, *Cd_E2*, *Cd_E3* (Variations of energy formulations)	Dimensionless
Cn	Drag coefficient for flow normal to disc/net panel, per Hansen (2008), equals Cd_{cyl} at $\varphi = 90°$	Dimensionless
β	Porosity, defined as $1 - Sn$	Dimensionless

3 Theory

This section derives the updated drag and flow reduction models for aquaculture nets in AquaSim, integrating one-dimensional momentum theory with existing formulations. We define net solidity, model drag forces and coefficients, analyze velocity reduction, and present a new drag coefficient for AquaSim 2.20 (2025), validated in later sections.

3.1 Solidity of Net Panels

Figure 3 shows a mathematical description of a net, as seen perpendicularly to the net.

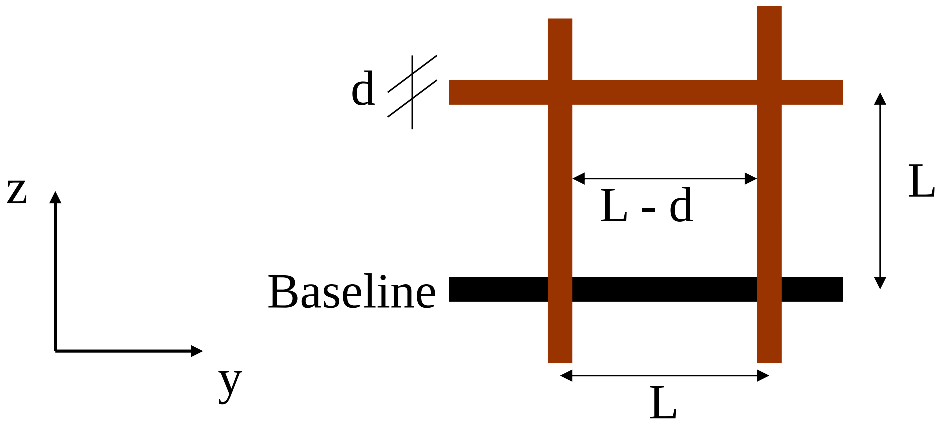

Figure 3 Twines in net. One twine denoted as baseline (from Berstad et. al. 2012).

In NS 9415 (2021), Solidity (Sn) is defined as "the relationship between the planned netting area and total area of a net panel" meaning $Sn = {}^{A_e}/_{A_{tot}}$, where A_e is the projected area of net twines and A_{tot} is the total area of the net panel including . For an ideal knotless mesh as shown in Figure 3 a mathematical expression for *Sn*, Sn_m can be formulated as in Equation 1):

$$Sn_m = \frac{2d}{L} - \frac{d^2}{L^2} \tag{1}$$

Historically, meshes were made with knots. This leads to higher solidity Sn_{kn} due to extra net material at the knots. An expression having been used by e.g. (Løland, 1991) is:

$$Sn_{kn} = \frac{2d}{L} + \frac{kd^2}{L^2} \tag{2}$$

Here k is a constant, typically 1 or 2. Another simplified definition for solidity, Sn_{2d} is found as:

$$Sn_{2d} = \frac{2d}{L} \tag{3}$$

This is often denoted the "2D solidity" since it basically found by the summation of diameters in both directions. This can be a good balance since most nets are not mathematically perfect, with an example seen in Figure 2, and is in accordance with NS 9415 (2021) pp 112: "In the case of nettings with square meshes, solidity shall be determined, either to be twice the twine thickness divided by the mesh side, or with use of image processing".

The solidity of a net is the base for establishing the drag coefficient, Cd expresses the relation between F_{drag} and an undisturbed free-stream velocity, v.

$$F_{drag} = \frac{1}{2}\rho Cd A v^2 \tag{4}$$

ρ is the fluid density and Cd is the drag coefficient. A is an area consistent with the drag coefficient, often the cross-flow area. In this paper the area, A, corresponds to the total area of the net panel, A_{tot}, unless otherwise stated. Also, all flow directions are perpendicular to the net. In cases where the net is not fixed, the velocity, v, is the relative velocity between the fluid and the net.

3.2 Velocity reduction behind nets

Løland (1991) proposed a relationship between the solidity of net and the velocity reduction behind the net, r_L as:

$$r_L = 1 - 0.46Cd \tag{5}$$

Where r_L express the flow velocity behind the net relative to the undisturbed velocity.

This paper presents a reduction factor for flow behind a net based on 1-D Momentum theory (Rankine (1865), Froude (1878), Glauert (1935)). This paper follows the description in Hansen (2008). The 1-D Momentum theory considers flow through a permeable disc with solidity Sn as shown in Figure 4. A disc perpendicular to, and axis-symmetric about the x-axis is assumed. An incident flow along the x-axis with an undisturbed free-stream velocity, v, occurs as shown in Figure 4. There will be a reduced flow velocity, v_{red}, behind the net, and a velocity, u, at the net, as shown in the figure.

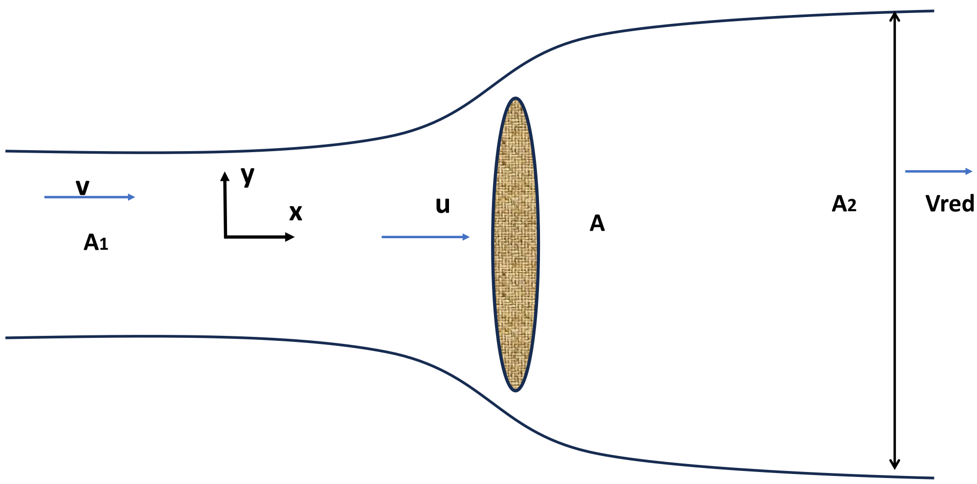

Figure 4 Flow through disc symmetric about the central axis.

A net is not axis symmetric similar to a disc, but for a large net one may use such an estimate both in the large global scale, but also in a smaller local scale as shown in Figure 5. Intuitively one may assume that Figure 4 can describe the local situation seen in Figure 5 for low solidity and a global situation for high solidity.

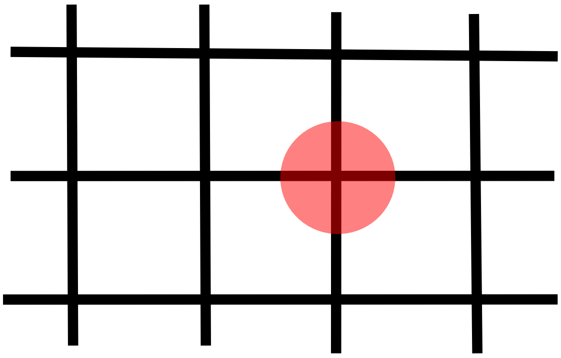

Figure 5 Net twines with a local disc indicated.

The disk in Figure 4 will have a pressure drop over it, leading to a force (drag) pushing in the direction of the flow. In the vocabulary of Hansen, the drag force corresponds to the thrust force, T. Following Glauert (1935), by putting up the applicable control volume, Hansen (2008) ends up with Eq 4.12 and shows that the drag force to the disc in Figure 4 is:

$$T = F_{drag} = \rho u A (v - v_{red}) \tag{6}$$

Where u, is the flow velocity at the disc, as illustrated in Figure 4. A is the total area that the disc covers normal to the flow. The flow velocity, u, at the disc will be, according to Hansen (2008) Eq. 4.11:

$$u = \frac{1}{2}(v + v_{red}) \tag{7}$$

By inserting Equation (7) into Equation (6) it is seen that the drag force can be expressed as

$$F_{drag} = \frac{1}{2}\rho A (v + v_{red})(v - v_{red})$$

meaning

$$F_{drag} = \frac{1}{2}\rho A (v^2 - {v_{red}}^2) \tag{8}$$

By definition, the drag coefficient expresses the relation between F_{drag} and an undisturbed free-stream velocity, v as given in Equation (4)

Combining Equation (8) and Equation (4) means:

$$\frac{1}{2}\rho A (v^2 - {v_{red}}^2) = \frac{1}{2}\rho C d A v^2$$

Meaning

$$v^2 - {v_{red}}^2 = C d v^2$$

Meaning

$${v_{red}}^2 = v^2 (1 - Cd)$$

Meaning

$$v_{red} = v\sqrt{1 - Cd} \tag{9}$$

Meaning the current reduction factor r_E, will be:

$$r_E = \frac{v_{red}}{v} = \sqrt{1 - Cd} \tag{10}$$

This method for deriving the reduction of the flow velocity behind the net with reduction factor r_E will be denoted the "Energy method" in this paper. This is also how this method is denoted in AquaSim.

3.3 Comparison energy relation and Lølands formulae

Figure 6 compares the reduction factor by Løland, r_L, to the reduction factor, $r_{E,}$ stemming from the energy method.

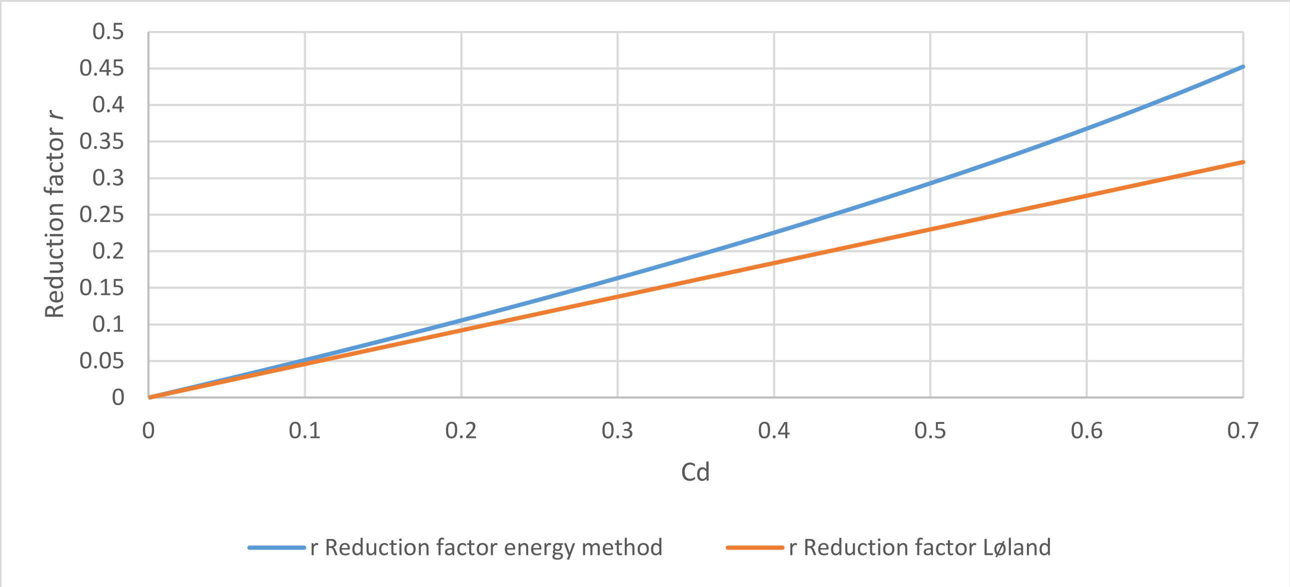

Figure 6 Comparison between r_L and r_E as function of the drag coefficient, Cd.

As seen from Figure 6 the reduction predicted by the energy method is higher than from the Løland method, in particular for higher drag coefficients.

3.4 Drag coefficient for turbines

The application in Hansen (2008) is turbine blades as shown Figure 7. Consider a section of the blade as seen in the figure. When turbine blades rotate around its central axis, the section will cover a circle as marked in white in the figure. The solidity is defined as the ratio between how much area is covered by blades relative to the total area covered by the circle. This definition is analogous to the definition of solidity for nets.

Figure 7 Turbine blade.

Hansen (2008), Eq. 4.15 introduces a relation between the undisturbed free-stream velocity, *v,* and the velocity at the disc, *u,* as an "induction factor", *a,* where the velocity at the net, *u*, can be expressed with the following relation:

$$u = v(1 - a) \tag{11}$$

Where *a* is related to a drag coefficient, Hansen (2008) Eq. 4.23:

$$Cd = 4a(1 - a) \tag{12}$$

Furthermore, Hansen (2008) defines a solidity, σ, as the fraction of the annular area in the control volume which is covered by blades. This is defined as *Sn* for nets. The inflow angle ϕ is defined with $\phi = 90^o$ corresponding to a direction normal to the disc/net panel. The drag coefficient for flow normal to the disc/net panel is defined as C_n, which for $\phi = 90^o$ means $C_n = Cd_{cyl}$, according to Hansen (2008) Eq. 6.12. Eq. 6.23 in Hansen (2008) states:

$$a = \frac{1}{\frac{4\sin^2\phi}{\sigma C_n} + 1} \tag{13}$$

Translating Eq. 6.23 in Hansen (2008) to the vocabulary of this paper yields:

- $\sigma = Sn$
- $C_n = Cd_{cyl}$
- $Sin^2\phi = 1$

This means that for the net considered in Figure 4, *a* can be expressed as,

$$a = \frac{1}{\frac{4}{SnCd_{cyl}} + 1} \tag{14}$$

Using $Cd_{cyl} = 1$, which is the basis in AquaSim, means *a* can be expressed as,

$$a = \frac{1}{\frac{4}{Sn} + 1} \tag{15}$$

or

$$a = \frac{Sn}{4 + Sn} \tag{16}$$

Inserting Equation (16) into Equation (12) gives:

$$Cd = 4\frac{Sn}{4 + Sn} * (1 - \frac{Sn}{4 + Sn}) \tag{17}$$

$$Cd = \frac{Sn}{\left(1 + \frac{Sn}{4}\right)^2} \tag{18}$$

As seen from Equation (18), the drag coefficient relative to solidity is decreasing by increasing solidity. This does not fit with empirical data for nets but seems plausible for turbines where the solidity close to the nave will be high, and incoming wind will be led radially outwards.

3.5 Drag coefficient for net panels

In Berstad et al. (2012) an assessment is made by considering the difference between water flowing past a single twine (black in Figure 3), versus flowing past a single twine with additional obstacles, i.e. the brown twines in Figure 3. It presents a relation between the drag for a flow past a single twine, and the drag for a perpendicular flow through a net, as shown Figure 8.

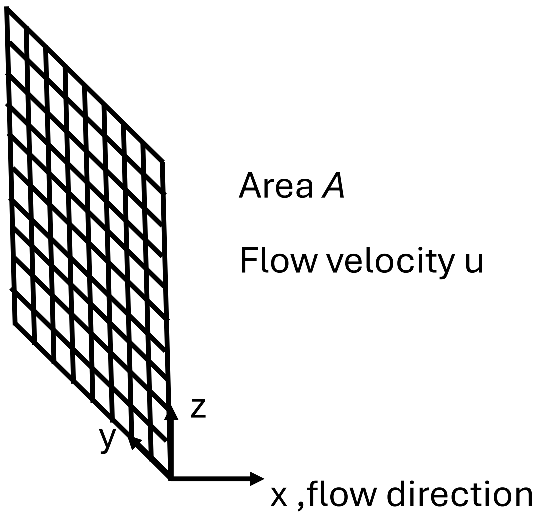

Figure 8 Panel in the yz-plane with water flowing through, having an area, A, perpendicular to the flow. The flow is along the x-axis.

In Berstad et al. (2012), the drag coefficient is defined relative to the area of twines only, A_e. Relating the *Cd* to the total area of the panel, A_{tot}, leads to:

$$Cd_{2012} = Cd_{cyl} \frac{Sn}{(1 - \frac{Sn}{2})^3} \tag{19}$$

Cd_{cyl} is the applicable drag coefficient if only a single twine was considered to be present in the flow. As a default $Cd_{cyl} = 1$, which means that:

$$Cd_{2012} = \frac{Sn}{(1 - \frac{Sn}{2})^3} \tag{20}$$

The drag coefficient formula for drag in a net relative to drag around a solitary twine in Berstad et al. (2012) is based on the local flow velocity at the immediate front, *u*, of the net as seen from Figure 8. The Berstad et al. (2012) paper assumes $u = v$, and does not assess how the flow, *u*, relates to an undisturbed flow further upstream of the net, *v*. This means that the drag given by the 2012 version can be expressed by,

$$F_{drag} = \frac{1}{2} \rho Cd_{2012} A \frac{u^2}{v^2} v^2 \tag{21}$$

when applying the undisturbed free-stream velocity, *v*. Combining Equation (21) and the definition of *Cd* related to undisturbed flow from Equation (4), leads to the following expression for *Cd*:

$$Cd = Cd_{2012} \left(\frac{u}{v}\right)^2 \tag{22}$$

Meaning:

$$Cd = \frac{Sn}{(1-\frac{Sn}{2})^3}\frac{u^2}{v^2}$$

(23)

From Equation (7) (Hansen (2008) Eq. 4.11) the velocity at the panel is the average of the undisturbed velocity and the reduced velocity, hence:

$$u = \frac{v}{2} + \frac{v_{red}}{2} = \frac{v}{2} + \frac{v\sqrt{1-Cd}}{2} = \frac{v}{2}\left(1+\sqrt{1-Cd}\right)$$

(24)

Meaning that:

$$\frac{u}{v} = \frac{1}{2} + \frac{\sqrt{1-Cd}}{2}$$

(25)

$$\frac{u^2}{v^2} = \left(\frac{1}{2} + \frac{\sqrt{1-Cd}}{2}\right)^2$$

$$Cd = \frac{Sn}{(1-\frac{Sn}{2})^3}\left(\frac{1}{2} + \frac{\sqrt{1-Cd}}{2}\right)^2$$

Solving this for Cd Means,

$$Cd\_\mathrm{E1} \quad = \frac{Sn}{(1-\frac{Sn}{2})^3}\frac{1}{\left(1+\frac{Sn}{4(1-\frac{Sn}{2})^3}\right)^2}$$

(26)

in case $Cd_{cyl} = 1$. For a general Cd_{cyl}, the expression becomes,

$$Cd\_\mathrm{E1} \quad = \frac{SnCd_{cyl}}{(1-\frac{Sn}{2})^3}\frac{1}{\left(1+\frac{SnCd_{cyl}}{4(1-\frac{Sn}{2})^3}\right)^2}$$

(27)

when correcting for the effect of the average velocity, *u*. This correction is based on the Hansen (2008) relation between solidity and *Cd.* Using the *Cd* derived by Hansen (2008) as basis for this correction could be appropriate. In this case,

$$\frac{u}{v} = (1-a)$$

(28)

and hence,

$$\frac{u^2}{v^2} = (1-a)^2$$

(29)

This means Equation (23) can be expressed as,

$$Cd = \frac{Sn}{(1-\frac{Sn}{2})^3}(1-a)^2$$

(30)

Following the Hansen (2008) relation between solidity, *Sn*, and the "induction factor", *a*, from Equation (16), the drag coefficient, *Cd* can be expressed as,

$$Cd\_E2 \quad = \frac{Sn}{(1-\frac{Sn}{2})^3}\left(1-\frac{Sn}{4+Sn}\right)^2 \tag{31}$$

which is then the second possibility for correction. Making a Taylor series expansion at $Sn = 0$ of the correction, keeping the two first terms yields,

$$\left(1-\frac{Sn}{4+Sn}\right)^2 \approx 1-\frac{Sn}{2} \tag{32}$$

Such that a simplified expression for *Cd* can be expressed as,

$$Cd\_E3 \quad = \frac{Sn}{(1-\frac{Sn}{2})^2} \tag{33}$$

Figure 9 shows *Cd* derived from Equation (26), Equation (31) and Equation (33) respectively, compared to the polynomial fit proposed by Moe Føre et al. (2022) and the 2012 AquaSim formulation:

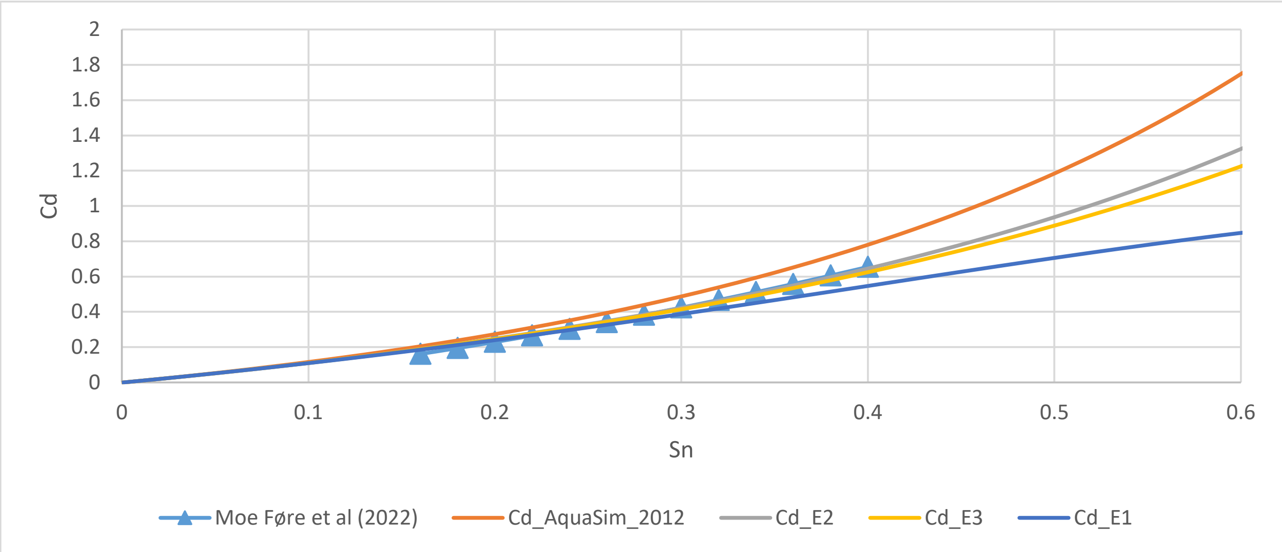

Figure 9 Cd as function of solidity.

In Figure 9:

- Moe Føre et al (2022): Proposed polynomial curve fit from Eq. 10 in Moe Føre et al. (2022).
- Cd_AquaSim_2012: The relation between solidity and drag coefficient in AquaSim 2012-2024.
- Cd_E2 = AquaSim 2025: The curve chosen for AquaSim 2025 (Equation (31)).
- Cd_E3: A simplified expression of Cd_E2, presented in Equation (33).
- Cd_E1: Drag coefficient outlined in Equation (27) ($Cd_{cyl} = 1$).

As seen from Figure 9, *Cd_E2* is the most conservative version of the equations using $Cd_{cyl} = 1$. If Cd_{cyl} is not *1*, then Equation (31) is:

$$Cd = \frac{Cd_{cyl}Sn}{(1-\frac{Sn}{2})^3}\left(1-\frac{Cd_{cyl}Sn}{4+Cd_{cyl}Sn}\right)^2 \tag{34}$$

4 EMPIRICAL DATA

Since 2012, the amount of empirical data has increased. This paper covers a few papers as presented in succeeding sections.

4.1 Moe Føre et al. (2022)

Moe Føre et al. (2022) covers a range of testing carried out both for flow perpendicular to nets and for flow at oblique angles. The data in Table 1 stems from this paper.

Table 1 Empirical data Moe Føre et al. (2022).

Solidity	No 1	No 2	No 3	No 4	No 5	No 6
0.185	0.205	0.215	0.22			
0.195	0.23	0.24				
0.2	0.215	0.22				
0.255	0.32	0.33	0.34	0.35		
0.33	0.46	0.48	0.51	0.53	0.54	0.57
0.365	0.56	0.57	0.6			

Figure 10 shows the data in Table 1 where the following is shown.

- The blue dots show test data.
- The red line shows a polynomial fit proposed by Moe Føre et al. (2022). The polynomial curve is given by: $Cd = 1.872Sn^2 + 1.057Sn - 0.053$ (Moe Føre et al. (2022) Eq. 10). The paper states that this polynomial fit is applicable for solidities, Sn, in the range [0.18-0.36]. Therefore the line is limited to this range.

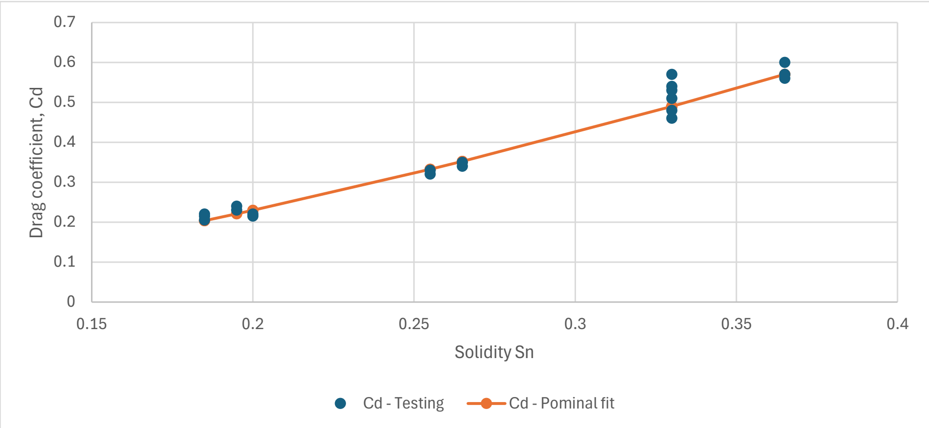

Figure 10 Drag as a function of solidity from Moe Føre et al. (2022).

4.2 Marchand et al. (2024)

Marchand et al. (2024) considered three-dimensional flow around and through a porous panel in a wind tunnel and created a large amount of empirical data where the data with Reynold number above approximately 50 is shown in Table 2.

Table 2 Empirical data Marchand et al. (2024).

	Solidity	No 1	No 2	No 3	No 4	No 5	No 6	No 7	No 8	No 9
P1	0.58	0.872	0.625	0.608	0.604	0.607				
P2	0.41	0.567	0.568	0.573	0.559	0.552				
P3	0.87	0.957								
P4	0.61	0.922								

P6	0.61	0.935								
P7	0.45	0.705								
P8	0.7	0.986								
P10	0.11	0.146								
P11	0.37	0.596	0.499	0.489	0.463	0.465				
P12	0.31	0.459	0.46	0.469	0.45	0.436				
P13	0.17	0.21								
P14	0.24	0.328								
P15	0.24	0.336								
P16	0.24	0.343								
P17	0.15	0.198								
P18	0.28	0.358								
P19	0.52	0.803								
P20	0.42	0.632								
P21	0.32	0.406								
P22	0.65	0.956								
P23	0.82	0.951								
P24	0.75	0.96								
P26	0.405	0.594	0.574	0.559	0.552	0.544				
P27	0.115	0.163	0.158	0.155	0.156	0.154	0.148	0.146	0.136	0.139
P28	0.114	0.139	0.139	0.136	0.132	0.129				
P30	0.08	0.088	0.085	0.088	0.092	0.087	0.086	0.08	0.083	0.079

The porous panels in Marchand et al. (2024) look similar to regular nets used in aquaculture.

4.3 Steiros et al. (2018)

Steiros et al. (2018) considers porous plates meaning they come from a culture where porosity, β, is defined as *1 - Sn*. They have conducted testing in water, with plates with circular openings, where their empirical data with the new empirical data being marked separately with 3 cases with relevant solidity as shown in Table 3.

Table 3 Empirical data, Steiros et al. (2018).

Solidity	Cd
0.4	0.76
0.5	1
0.6	1.1

Steiros et al. (2018) also propose a drag coefficient, given by,

$$Cd = u^{*2}\left(\frac{1}{(1-Sn)^2} - 1\right) - \frac{4}{3}\frac{(1-u^*)^3}{(2-u^*)^2}$$

Equation 35

Here u* is the velocity at the panel. This is estimated from Equation (7) in this paper and presented in Figure 11.

5 COMPARISON OF CURVES AND EMPIRICAL DATA

Figure 11 shows a comparison of empirical data and proposed relationships between solidity and *Cd*. The curves presents the following:

- Moe Føre et al (2022) curve: Proposed polynomial curve fit from Eq. 10 in Moe Føre et al. (2022).

- AquaSim 2012: The relation between solidity and drag coefficient in AquaSim 2012-2024.
- Cd_E2 : AquaSim 2025: The curve chosen for AquaSim 2025 Equation (31).
- Cd_E1: Drag coefficient outlined in Equation (27) ($Cd_{cyl} = 1$).
- Hansen (2008): Drag coefficient for the turbine considered by Hansen (2008).
- Steiros et al (2018) curve: The curve deducted from Steiros et al. (2018).
- Moe Føre et al (2022) Data: The empirical data from Moe Føre et al. (2022), Table 1.
- Marchand et al (2024): Empirical data deducted from Marchand et al (2024), Table 2.
- Steiros et al (2018) data: Empirical data deducted from Steiros et al. (2018).

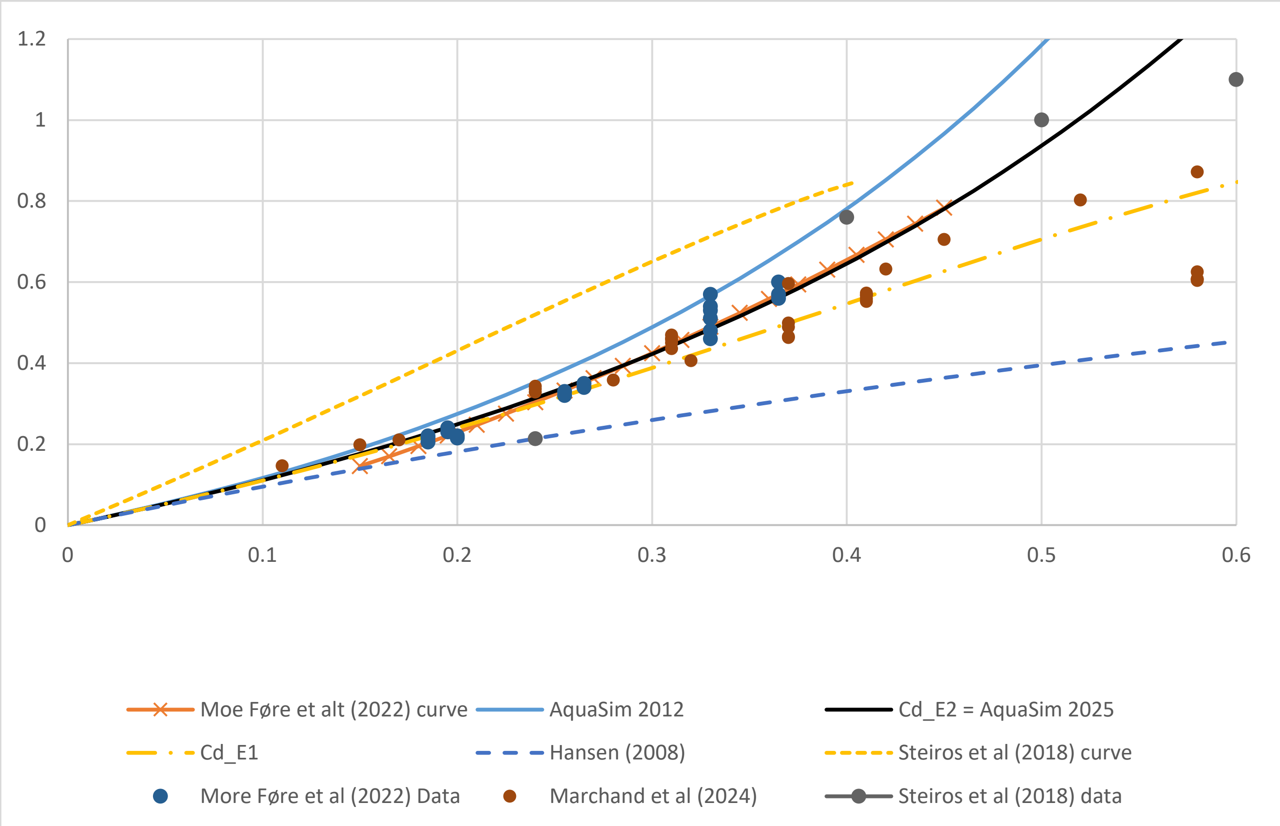

Figure 11 Comparison of empirical data and proposed relationships between solidity and Cd.

As seen from Figure 10 and Figure 11, The polynomial fit proposed by Moe Føre et al. (2022) provides a smooth trend derived from empirical data (Table 1 in Moe Føre et al. (2022)). The historical AquaSim curve (2012–2024) is on the conservative side of the Moe Føre et al. (2022) curve, whereas the new AquaSim 2025 curve fits very well with the Moe Føre et al. (2022) curve. This highlights the evolution in the prediction of *Cd* as more empirical data has arrived. As seen from Figure 11, the AquaSim 2025 curve is less conservative than the historical AquaSim curve (2012–2024), particularly for high solidities.

In addition to showing very good correspondence to the polynomial fit curve presented by Moe Føre et al. (2022), the AquaSim 2025 curve, also compares well to the Marchand et al. (2024) data, whereas the Cd_E1 curve will be non-conservative, as seen in Figure 12.

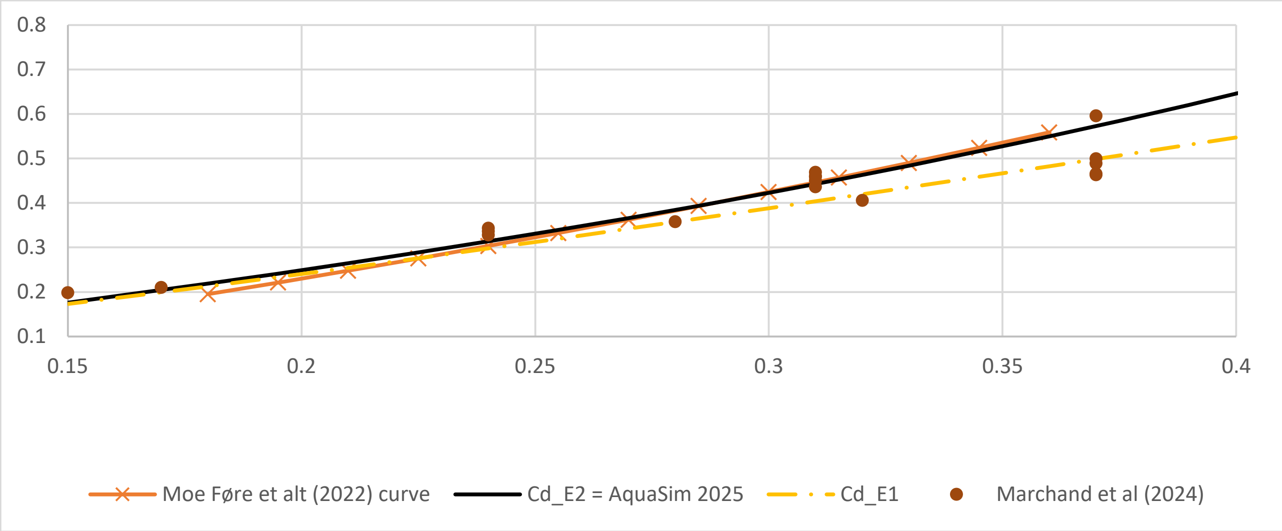

Figure 12 Drag as a function of solidity from Moe Føre et al. (2022), compared to AquaSim 2025.

The Cd_E1 curve seems promising as it shows lower Cd for very high solidity and may be a future possibility for implementation in AquaSim, as it does not increase as extremely as both the AquaSim 2012 curve and the AquaSim 2025 curve. In Figure 11, the Cd_E1 curve is based on $Cd_{cyl} = 1$, which may be increased if more empirical data arrive for the high solidity range, and one would not want less conservatism for the low solidity range.

If future empirical data show that the Cd_E1 curve is better for solidities above 0.4, then it may be combined with a $Cd_{cyl} > 1$, to fit with the empirical data in the 0.2–0.4 range.

The empirical data from multiple sources—Moe Føre et al. (2022), Marchand et al. (2024), and Steiros et al. (2018)—provide crucial validation points. These datasets capture real-world drag behavior across different experimental setups, supporting or challenging the theoretical and numerical curves.

Notably, the Steiros et al. (2018) curve presents a distinct trajectory with higher drag relative to solidity. Their work is generally more focused on very high solidity and plates with circular openings, so until more empirical data arrives, their work will not be included to influence the AquaSim default curve. Similarly, Hansen (2008) offers an independent assessment, specifically in the context of turbine drag characteristics. Although enriching the dataset, it represents a different setup and is not used to influence the AquaSim default curve.

The overall comparison reveals areas of agreement as well as divergence. Focusing on the data from Moe Føre et al. (2022) and Marchand et al. (2024), the curve chosen for AquaSim seems the most reasonable choice at this time.

6 CONCLUSIONS

This paper used energy relations to propose an energy-consistent relationship between drag forces to a net and the reduction of flow velocity behind the net as:

$$r_E = \sqrt{1 - Cd}$$

This paper also compares multiple approaches for modeling *Cd* as a function of solidity and it is concluded that the relation between solidity and drag to a net chosen for AquaSim 2025 fits well with empirical data.

ACKNOWLEDGEMENTS

This work was supported by the Norwegian Research Council, whose contribution is gratefully acknowledged.

References

Aquastructures (2013) “The AquaSim Package Theory User Manual” Aquastructures, Kjøpmannsgata 21, Trondheim, Norway. https://aquasim.no/files/documentation/Theory_manual.pdf

Aquastructures (2024) “Calculation of loads on turbine blades using BEM theory”. Aquastructures, Kjøpmannsgata 21, Trondheim, Norway. https://aquasim.no/resources/documentation.html . https://aquasim.no/files/validation/TR-FOU-100004-5-Rev4-BEM.pdf

Berstad, A. J., Walaunet, J., and Heimstad, L. F., (2012). “Loads from currents and waves on net structures”. 27th International Conference on Offshore Mechanics and Arctic Engineering, June 15-20. Rio, Brazil

Moe Føre, Heidi Moe, Per Christian Endresen & Hans V. Bjelland (2022) "Load Coefficients and Dimensions of Raschel Knitted Netting Materials in Fish Farms" Journal of Offshore Mechanics and Arctic Engineering AUGUST 2022, Vol. 144 / 041301-1.ASME,

Froude, W. (1878). "On the Elementary Relation between Pitch, Slip, and Propulsive Efficiency," Transactions of the Institution of Naval Architects, which introduced the actuator disc concept for propellers.

Glauert, H. (1935). Aerodynamic Theory: A General Review of Progress Under a Unified Notation, Volume IV, Division L ("Airplane Propellers"). Edited by W. F. Durand. Published by Springer (originally Julius Springer, Berlin).

Grieg (2023) https://www.radionordkapp.no/nyheter/24413/restauksjon-pa-oppdrett-i-finnmark/

Hansen, M. O. (2008). Aerodynamics of wind turbines. ISBN-13: 978-1-84407-438-2008

Løland, G., (1991). Current Forces on and Flow Through Fish Farms. Doktor ingeniøravhandling: Norges Tekniske Høgskole. Division of Marine Hydrodynamics, the Norwegian Institute of Technology

Marchand, Olivier C., Sophie Ramananarivo1, Camille Duprat and Christophe Josserand (2024) “Three-dimensional flow around and through a porous panel” J. Fluid Mech. (2024), vol. 987, A20, doi:10.1017/jfm.2024.372. Cambridge University Press.

Rankine, W. J. M. (1865). On the mechanical principles of the action of propellers. Transactions of the Institution of Naval Architects, 6, 13–39.

Standard Norway. NS 9415:2021: Floating fish farming installations – Requirements for design, dimensioning, production, installation, and operation. Lysaker: Standard Norway; 2021.

Steiros, K. and M. Hultmark (2018) "Drag on flat plates of arbitrary porosity" J. Fluid Mech. (2018), vol. 853, R3, doi:10.1017/jfm.2018.621. Cambridge University Press.